ISBN: 978-3-95450-231-8 ISSN: 2673-5490 doi: 10.18429/JACoW-IPAC2023-THPA009

OPTICAL PEPPER-POTS: DEVELOPING SINGLE-SHOT EMITTANCE DIAGNOSTICS

J. Wolfenden*, C. Swain, C. P. Welsch, University of Liverpool/Cockcroft Institute, UK
T. H. Pacey, ASTeC/Cockcroft Institute, STFC Darebury Laboratory, Sci-Tech Daresbury, UK

Abstract

Emittance measurements are a universal requirement when operating particle accelerators. Many techniques exist to achieve these measurements, each suiting the specific requirements of a machine. Most are multi-shot or invasive, and struggle to function with low energy beams or where space-charge effects are dominant. Generally, these limitations can be restricting, but especially so in emerging sectors such as novel acceleration or energy recovery linacs. To this end, two all-optical single-shot emittance measurements are being developed. In both cases the measurement is analogous to an optical version of the common pepper-pot diagnostic. The two methods are complementary: the first uses a micro-lens array (MLA); the second a digital micro-mirror device (DMD). Both systems can operate away from a beam waist and separate the optical beam radiation into beamlets rather than the beam itself; leaving potential for a non-invasive measurement. The benefits of using optical beam radiation are reduced beam scattering, simple designs, and suitability for low-energy/space-charge dominant beams. Presented is a series of benchmarking measurements and simulations with laser sources. Initial beam simulations, plans for first measurements, and the application to a machine learning virtual diagnostic are also discussed.

INTRODUCTION

A key feature of all applications of accelerated particle beams is emittance, ϵ. This is an approximation of the total volume a particle bunch occupies in 6D phase space [1]. This factor must be optimised to the application of the particle beam; for example, to achieve high novel acceleration gradients, injection and storage within synchrotrons, accurate dose delivery for therapy, and in high energy physics experiments. There are a range of methods to achieve this measurement depending on the facility and operational constraints. Most methods require multiple measurements with different beam optics [2], assuming a certain level of beam stability from shot-to-shot. Most are also invasive, involving the application of masks to a beam [3] or scanning beam optics settings [4], meaning a bunch cannot be used during measurements, and assuming stability once the diagnostic is removed from the beam path. Space charge can also interfere with these existing techniques, by obscuring or changing the actual value during the measurement process [5].

Optical alternatives to existing techniques offer a solution to these issues. Non-invasive and minimally invasive radiation production allows online operation and monitoring [6,7]. By masking optical radiation rather than the beam, interference from space charge on the measurement can be avoided. Two methods will be presented in this contribution; one using an MLA [8], as an optical pepper-pot measurement, and one using a DMD [9], for an optical pinhole/slit scanning technique. Both systems can produce a phase space reconstruction and the emittance. Neither system requires a special operational mode to conduct measurements, further reducing impact on beam operations.

This work will focus on the application of these techniques to transition radiation (TR). TR is used due to ease of generation and simulation during this initial development phase. TR is produced when the electric field of a charged particle traverses the boundary between two different dielectric constants [10]. Optical TR (OTR) is a purely surface effect, meaning it can be produced using extremely thin foils; for higher energy applications these foils can be used online with minimal impact on the beam [6].

LASER SIMULATION BENCHMARK

Prior to beam measurements with OTR, the measurement and analysis procedure of these two methods is being developed using a laser source. A laser is analogous to the highly directional OTR produced by a relativistic particle bunch. The transverse emittance of a laser can be calculated by treating the laser mathematically as a particle beam. It can be shown [1] that the beam transfer matrix for a focusing element followed drift is:

$$\Sigma_F = M\Sigma_I M^T, \tag{1}$$

with,

$$\begin{aligned}\Sigma_F &= \epsilon \begin{pmatrix} \beta_F & -\alpha_F \\ -\alpha_F & \gamma_F \end{pmatrix} = \begin{pmatrix} \sigma_{F,11} & \sigma_{F,12} \\ \sigma_{F,12} & \sigma_{F,22} \end{pmatrix} \\ &= \begin{pmatrix} < x^2 >_F & < xx' >_F \\ < xx' >_F & < x'^2 >_F \end{pmatrix}.\end{aligned} \tag{2}$$

Here indices I and F indicate the initial and final positions of the transfer matrix, Σ is the beam matrix as defined by Equ. 2, with Twiss parameters α, β, and γ. The beam transfer matrix M is defined by the path between I and F; in this case, this is composed of a lens of focal length, f followed by a drift, L,

$$M = \begin{pmatrix} 1 & L \\ 0 & 1 \end{pmatrix} \begin{pmatrix} 1 & 0 \\ -1/f & 1 \end{pmatrix} \tag{3}$$

Equation 2 shows how the beam matrix can be related to the measurable parameters of the beam. These beam matrix parameters can then be substituted into:

$$\epsilon = \sqrt{\sigma_{11}\sigma_{22} - \sigma_{12}^2}, \tag{4}$$

* joseph.wolfenden@cockcroft.ac.uk

ISBN: 978-3-95450-231-8 ISSN: 2673-5490 doi: 10.18429/JACoW-IPAC2023-THPA009

to calculate emittance. Equ. 4 can be calculated by solving Equ. 1 with Equ. 3 and grouping the terms by factors of L:

$$\sigma_{F,11} = \left(\frac{\sigma_{I,11}}{f^2} - 2\frac{\sigma_{I,12}}{f} + \sigma_{I,22}\right) L^2 + 2\left(\frac{-\sigma_{I,11}}{f} + \sigma_{I,12}\right) L + \sigma_{I,11}. \quad (5)$$

Fitting Equ. 5 to a multi-screen-type measurement of the laser [2], a phase space ellipse and emittance can be defined. From optical theory [11], the propagation of a Gaussian laser can be defined as:

$$\omega^2 = \omega_0^2 + \left(\frac{\lambda}{\pi\omega_0}\right)^2 z^2 \quad (6)$$

where ω is the 2σ waist of the laser, σ being the square-root of the profile variance $\left(\sqrt{< x^2 >}\right)$, ω_0 is the minimum waist value at the focus, λ is the laser wavelength, and z is the longitudinal propagation distance. It is clear to see that by defining $L = z$ Equ. 6 is already in the same format as Equ. 5. Solving for the three matrix components, choosing a wavelength (532 nm) and substituting into Equ. 4 provides:

$$\epsilon = \frac{\lambda}{4\pi} = 0.042\,\text{mm mrad}. \quad (7)$$

Benchmarking work began with simulations of the laser measurement. Zemax OpticStudio [12] would be used to conduct the eventual OTR simulations, based on previous work [13], therefore this was used to propagate a pure Gaussian laser through a focussing element and along a drift region. Three lenses were chosen; a theoretical thin lens with $f = 100$ mm, a real lens (AC508-100-A [14]) with $f = 100$ mm, and a real lens (AC508-500-A [15]) with $f = 500$ mm. Profile measurements were taken along the optical axis of each system and then plotted. An example of the propagation results are provided in Fig. 1. These results were then combined

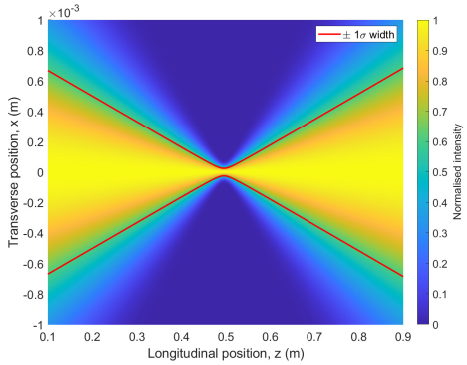

Figure 1: Example simulated laser image profile propagation along with the $\pm 1\sigma$ waist. This was for a AC508-500-A lens.

with Equ. 5, Equ. 4, and Equ. 2 to produce phase plots and emittances for each system. The results, along with those from theory, are presented in Fig.2. Despite the variation in the phase ellipse, which is expected given the different optical systems, the emittance is constant. This demonstrates

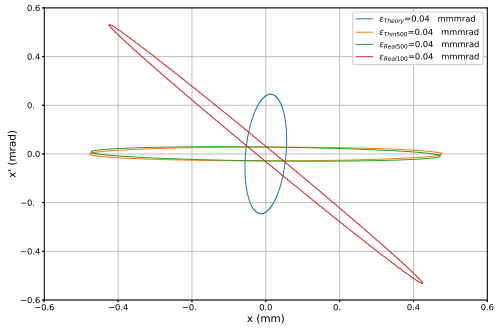

Figure 2: Simulated laser phase spaces and emittances.

the ability to consistently measure the emittance of a laser, providing a cross-check value between the MLA and DMD methods.

LASER SIMULATIONS

The next step was to simulate a simple MLA system with the same laser parameters. A schematic of this system is presented in Fig. 3. An image of the laser on the surface

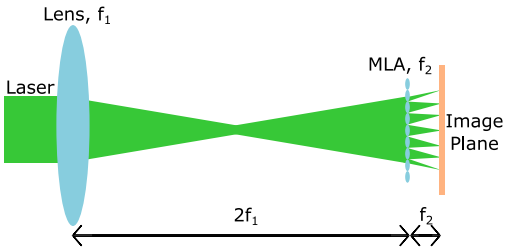

Figure 3: Schematic of the system for MLA simulations, and also to simulate the DMD setup, but replacing the lens positions with mask apertures.

of the MLA and the image in the focal plane of the MLA were collected. An example result is presented in Fig 4. The

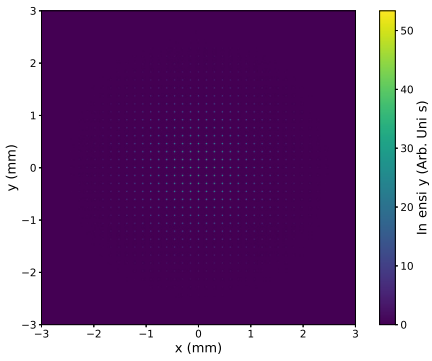

Figure 4: Example image from an MLA simulation.

analysis of these images is not too dissimilar to that of a standard pepper-pot system [5]. The main difference is how the σ' of the individual peaks in the image is defined. Rather than this being defined by the drift length, as in a standard

ISBN: 978-3-95450-231-8 ISSN: 2673-5490 doi: 10.18429/JACoW-IPAC2023-THPA009

beam-based measurement, as shown in Fig. 3 measurements occur in the focal plane of the MLA. Hence the angle is defined by the focal length of the MLA, and the emittance is therefore defined as:

$$\begin{aligned}\epsilon_x^2 &= \langle x^2 \rangle \langle x'^2 \rangle - \langle x x' \rangle^2 \\ &= \frac{1}{N^2}\left[\sum_{j=1}^{p} n_j \left(x_{sj} - \bar{x}\right)^2\right]\left[\sum_{j=1}^{p}\left[n_j \sigma_{x'_j}^2 + n_j \left(\bar{x'_j} - \bar{x'}\right)^2\right]\right] \\ &\quad - \frac{1}{N^2}\left[\sum_{j=1}^{p} n_j x_{sj} \bar{x'_j} - N\bar{x}\bar{x'}\right]^2,\end{aligned} \tag{8}$$

where N is the total number of photons, n_j is the number of photons in the j^{th} peak, p is the total number of peaks, x_{sj} is the position of the j^{th} micro-lens, $\bar{x}$ is the mean position all photons, $\bar{x'}$ is the mean divergence of all photons, $\bar{x'_j}$ is the mean divergence of all photons in the j^{th} peak, and $\sigma_{x'_j}^2$ is the variance of the j^{th} peak. Applying Equ. 8 to Fig. 4 provided the phase ellipse and emittance presented in Fig. 5. There is a very prominent difference to the results presented in Fig. 2. Upon further investigation it became apparent that

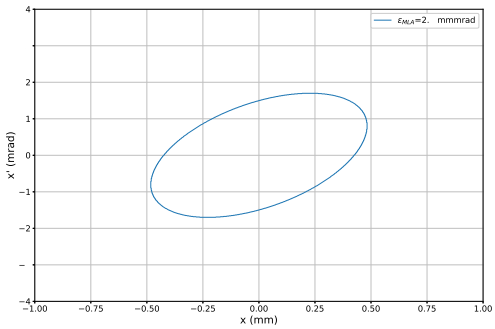

Figure 5: Phase space and emittance calculated from MLA images.

the width of the peaks in the MLA image were not varying as expected. The central peaks, where divergence is the lowest, should provide the narrowest peaks. In reality the peak widths were mostly constant aside from the very outer peaks. Comparing the individual peaks with the expected point spread function (PSF) [11] of an individual micro-lens, shown in Fig 6, it is clear that the peaks are diffraction limited. Therefore the micro-lenses are incapable of resolving the the divergence of a laser. OTR will provide a solution to this apparent resolution limit. The characteristic ring shape of the OTR means that the divergence is measured from a change in visibility of the peaks rather than a width [10]. The system resolution is then defined by the ability to monitor this visibility. As beam energy is increased, the OTR distribution narrows, and the visibility resolution increases. Resolution can also be increased by using larger micro-lenses; the lenses used in this study were ⌀150 µm, but ⌀300 µm or more are available off-the-shelf. This final point is linked to how a DMD could be used to provide much higher resolution. A larger "pinhole mask" would provide a narrower PSF, and hence higher resolution.

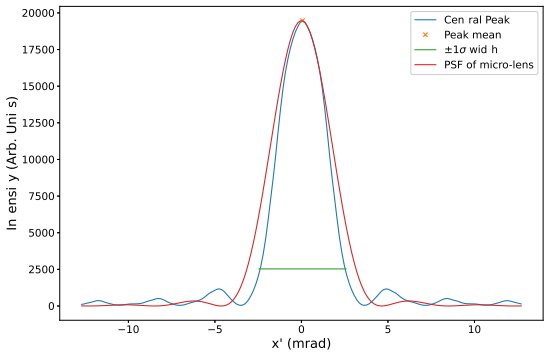

Figure 6: Comparison of MLA peak with micro lens PSF.

DISCUSSION AND FUTURE PLANS

End-to-end OTR simulations will be an important next step to demonstrate the viability of the MLA and DMD methods. Measurements with a laser source will also provide a reliable cross-check value across the DMD and MLA systems. Despite the diffraction limit, the result will be reproducible if DMD pinhole diameters are matched to the MLA apertures. Beam measurements with OTR are planned at CLEAR (CERN, CH) in the near future.

Following this, it would be straightforward to adapt this technology to image other, non-interceptive, radiation sources; this would make the technique non-invasive. A non-invasive single-shot method of measuring emittance would have applications across all accelerator sectors. This is particularly the case for novel acceleration where this system could be used to non-invasively monitor both pre-injection, and post-plasma accelerated electron beams.

Finally, work will commence to leverage existing experience of machine learning techniques to increase the insight a single image can provide, from advanced analysis, to machine control.

ACKNOWLEDGEMENT

This work is supported by the AWAKE-UK phase II project funded by STFC under grant ST/T001941/1 and the STFC Cockcroft Institute core grant ST/V001612/1.

REFERENCES

[1] H. Wiedemann, "Particle Accelerator Physics", 4th ed., Springer, 2015.

[2] M. Minty and F. Zimmermann, "Measurements and Control of Charged Particle Beams", Springer, 2003.

[3] J.G. Wang and D.X. Wang and M. Reiser. "Beam emittance measurement by the pepper-pot method", *Nucl. Instr. and*

ISBN: 978-3-95450-231-8 ISSN: 2673-5490 doi: 10.18429/JACoW-IPAC2023-THPA009

Meth. A. vol. 307(2), 190-194, Feb. 1991, doi:10.1016/0168-9002(91)90182-P

[4] K. Poorrezaei, R. Fiorito, R. Kishek, and B. Beaudoin, "New technique to measure emittance for beams with space charge", *Phys. Rev. ST Accel. Beams* 16, 082801, Aug. 2013, doi:10.1103/PhysRevSTAB.16.082801

[5] M. Zhang, "Emittance Formula for Slits and Pepper-pot Measurement", FERMILAB-TM-1988, Oct. 1996

[6] A. Faus-Golfe, J. Alabau Gonzalvo, C. Blanch Gutierrez, D. McCormick, J. Cruz, M. Woodley, and G. White, "Multi-OTR System for ATF2", *Physics Procedia* 37, 2072-2079, Oct. 2012, doi:10.1016/j.phpro.2012.02.525

[7] R. Fiorito, A. Shkvarunets, D. Castronovo, M. Cornacchia, S. Di Mitri, R. Kishek, C. Tschalaer, and M. Veronese, "Non-invasive emittance and energy spread monitor using optical synchrotron radiation", *Phys. Rev. ST Accel. Beams* 17, 122803, Dec. 2014, doi:10.1103/PhysRevSTAB.17.122803

[8] Fused Silica Microlens Arrays, Thorlabs Inc., `https://www.thorlabs.com/newgrouppage9.cfm?objectgroup_id=2861`, Accessed on: April 2023

[9] Digital Micro-mirror Device, Vialux GmbH, `https://www.vialux.de/en/superspeed-v-modules.html`, Accessed on: April 2023

[10] M. Ter-Mikaelian, "High Energy Electromagnetic Processes in Condensed Media", New York, J. Wiley - Interscience, 1972

[11] A. E. Siegmann, "Lasers", University Science Books, 1986

[12] Zemax OpticStudio, `www.zemax.com/products/opticstudio`, Accessed on: April 2023

[13] J. Wolfenden, R. B. Fiorito, and C. P. Welsch, "A novel simulation and analysis algorithm for high resolution optical transition radiation imaging", *Optics Express* 27 (3), 2988-2999, Jan. 2019, doi:10.1364/OE.27.002988

[14] AC508-100-A, `https://www.thorlabs.com/thorproduct.cfm?partnumber=AC508-100-A`, Accessed on: April 2023

[15] AC508-500-A, Thorlabs Inc., `https://www.thorlabs.com/thorproduct.cfm?partnumber=AC508-500-A`, Accessed on: April 2023